OPTOELECTRONICS AND ADVANCED MATERIALS – RAPID COMMUNICATIONS Vol. 6, No. 9-10, September – October 2012, p. 902 - 910

Study of electronic band structure and optical parameters of X-antimonides (X=B, Al, Ga, In) by modified Becke-Johnson potential

MASOOD YOUSAF, M. A. SAEED*, R. AHMED, M.M. ALSARDIA, AHMAD RADZI MAT ISA, A. SHAARI
Physics Department, Faculty of Science, Universiti Teknologi Malaysia, Skudai-81310, Johor, Malaysia

Electronic band structure and optical parameters of X-antimonides (X=B, Al, Ga, In) are investigated by first-principles FP-L (APW+lo) scheme of calculation based on a new exchange correlation potential approximation known as mBJ (modified Becke-Johnson). In this approach of exchange correlation approximation, excited states properties are dealt more accurately. Pattern of our calculated numerical band gap energy values is as follows: E_g(mBJ-GGA/LDA)> E_g(GGA) > E_g(LDA). The band gap values of InSb and AlSb are not only close to the experimental results but also realistic. A comprehensive analysis of linear optical parametric quantities (dielectric constant, refractive index, reflectivity and optical conductivity) related to electronic band structure is also presented. In our calculations, the first critical point (optical absorption's edge) is noted at about 1.136 eV, 1.804 eV, 1.331 eV, and 0.503 eV for BSb, AlSb, GaSb and InSb respectively. The present study suggests the use of these compounds in optoelectronic applications in different energy ranges.

(Received June 27, 2012; accepted September 20, 2012)

Keywords: Optical properties, DFT, FP-LAPW + lo, mBJ-GGA, Electronic structure, GGA-EV

1. Introduction

X-Antimonide (X= B,Al,Ga,In) binary compounds belonging to III-V semiconductors are important because of their useful electronic and optical properties. They crystallize in zinc blend structure at ambient conditions; characterize by a single lattice constant [1]. The band gap of BSb along with AlSb is indirect while that of GaSb together with InSb is direct [2].

III-Antimonides are under extensive study because of their multiple high technological applications such as anode material for lithium batteries [3-9]. They are also suitable for quantum wells [10], hetero-structures [10], diode lasers, LED's, mixing components for frequency, photo-detectors, and electro-optic modulators [1]. Antimonide compounds are used in advanced device applications due to high mobility [11]. BSb is a recommended for optical and electronic devices operating at elevated temperatures [2]. AlSb is ideally applicable for solar cells, high energy photon detectors [12] and optoelectronics based on $Ga_{1-x}Al_xSb$ [13]. For low radiator temperature systems, GaSb is better applicant for thermo-voltaic cells than Silicon as its cell technology is simpler and more efficient [2].

True evaluation of electro-optical parametric quantities is important for the devices. For this purpose, a recent technique namely modified Becke Johnson Potential (mBJ) is being employed for first time on these compounds which is known for overcoming the problem of band gaps' underestimation, in case of LDA (Local Density Approximation) [14] and GGA (Generalized Gradient Approximation) [15].

Previously, alternative form of GGA called as EV-GGA proposed by Engel and Vosko was used [2] to calculate band gap values of these compounds. In DFT, exchange correlation (functional) in addition to subsequent potential is a main contributor for overall energy estimations. Recently calculated direct band gap values [2] are underestimated compare to our calculated values. The difference between the present and other calculations is the use of mBJ potential which produces improved band gap results than ordinary LDA and GGA which calculate underestimating band gap values [16]. To address this issue, number of ways has been developed to reduce the difference between calculated and experimental value of material's band gap. Among these techniques, OEP (optimized effective potential) produces precise results as compared to theoretical and experimental studies [16, 17]. LDA+U [18] is another possibility but its implementation is not diverse. OEP and LDA+U methods are computationally expensive [16, 17].

Thus, to solve above mentioned dilemma matchless choice is the use of mBJ (exchange potential approximation) [19] that produces the band gap of

semiconductors and insulators in a precise way. A lot of previous studies support that mBJ gives better band gap results (very close to the experimental values) as compare to the LDA and GGA techniques [20, 21].

2. Method of calculations

We have carried out the computational work using the FP-LAPW+lo (Full potential linearized- augmented plane wave + local orbital) method under theoretical study of DFT [22] through recent version of WIEN2k computer package [23]. The mBJ (potential) was selected as it improves the judgment of band gap values as compared to LDA and GGA.

In the FP-LAPW scheme, a unit cell is divided into an atomic sphere (having specific radius known as RMT) and interstitial zone. Inside Atomic spheres known as muffin-tin (MT) the basis set is divided into two subsets: (1) core and (2) valence states. The core states are enclosed within MT sphere and have charge density in spherical symmetry [24]. Inside the MT spheres, the basis sets are solved as radial solutions of Schrodinger equation arranged linearly.

These calculations involve a parameter RMT*Kmax = 8 (determines the extent of the secular matrix), where the RMT is radius of MT sphere and K_{max} represents maximum K vector value in the first BZ (Brillion Zone). G_{max} was selected to be $14(Ry)^{1/2}$ which describes Fourier expansion of the charge density. (0, 0, 0) and (0.25, 0.25, 0.25) are the position of atoms in zinc blend structure which consists of two interpenetrating face centered cubic sub-lattices. The fallowing states $4d^{10}5s^{2}5p^{3}$, $4d^{10}5s^{2}5p^{1}$, $3d^{10}4s^{2}4p^{1}$, $3s^{2}3p^{1}$ and $2s^{2}2p^{1}$ for Sb, In, Ga, Al and B respectively are considered as valence electrons. The MT radii of Sb, In, Ga, Al and B, and are adopted to be 2.3, 2.4, 2.1, 2.0 and 1.5 (a.u) respectively. K-mesh accompanying 700 K-points in first Brillion zone integration within respective irreducible wedge is performed. A number of iterations (40) are dedicated to accomplish self consistency. For succeeding iterations, there is a total energy difference of less than 0.00001 Ry in per formula unit.

3. Results and discussions

The study involves comparison of electronic band structure with LDA, GGA and mBJ-GGA while optical traits (dielectric's real and imaginary part, refractive index, extinction coefficient, reflectivity and optical conductivity) of III-Antimonide compounds are presented with mBJ-GGA.

Firstly, optimum volume was obtained by minimizing the total energy with respect to the volume. By the use of Murnaghan equation of state (EOS) [25], optimized values of a_0 (lattice constants), B_0 (the bulk modulus) and B'(bulk modulus pressure derivative) are obtained and are listed in Table.1. It is clear from Table1 that our reported a_0 value for the compounds does not differ more than 1% from experimental values which shows a close agreement. Almost in all of band gap plots by LDA and GGA produce similar results and also in case of mBJ-GGA and mBJ-LDA similar behavior is observed. The unoccupied bands moved away from Fermi level in case of mBJ-GGA/LDA to enhanced band gap as compare to GGA/LDA with the similar shape and character of band structure.

Fig. 1 shows the calculated band structure of compounds with mBJ-GGA, mBJ-LDA, GGA and LDA. With GGA/LDA our band gap results are in good agreement with the results obtained by earlier GGA/LDA calculations while in case of mBJ-GGA/LDA enhanced band gap results are obtained over GGA/LDA calculated results [2]. It is clear from the figures that BSb & AlSb are indirect band gap and GaSb & InSb are direct band gap compounds. Direct band gap shows the optical activeness of materials, this feature can be utilized in photonic and optoelectronic applications [34]. In case of GGA/LDA, the band gap values for GaSb/InSb are closer to zero showing metallic behavior that is not true. The reason for not reporting the true nature of GaSb/InSb band gap might lie in the selection of exchange correlation functional in these approximations [2]. This means band gap results (1.331eV for GaSb and 0.503 eV for InSb) in case of mBJ-GGA are closer to the true instinct of GaSb/InSb. This is very important that the band gap calculated in the present study is much enhanced to other calculated band gaps of the herein studied material. The usage of mBJ potential has significantly improved the band gap values calculated with ordinary GGA/LDA [16]. In the present study band gap value (E_g) calculated with mBJ-GGA/LDA is greater than values obtained from GGA/LDA and are reported in Table 2.

Table 1. The lattice parameter (a), volume (V), bulk modulus (B) and its pressure derivative (B') of BSb, AlSb, GaSb, and InSb compounds.

Compounds	**Method**	**a (A°)**	**V $(a.u.)^3$**	**B (GPa)**	B'
BSb					
Present work	FP-LAPW-GGA	5.277	248.171	97.021	4.341
	FP-LAPW-LDA	5.188	235.845	110.832	4.579
Experiment	-	-	-	-	-
Other calculations	FP-LDA	5.191 [2]	-	111 [2]	4.36 [2]
	FP-GGA	5.279[2]	-	096 [2]	4.55 [2]
	PP-LDA	5.12 [26]	-	115 [26]	5.28 [26]
	PP-LDA	5.156 [27]	-	108 [27]	4.03 [27]
	FP-GGA	5.252 [28]	-	103 [28]	3.89 [28]
AlSb					
Present work	FP-LAPW-GGA	6.226	407.583	49.296	4.121
	FP-LAPW-LDA	6.108	384.875	55.695	4.379
Experiment	-	6.135 [29]	-	58 [29]	–
Other calculations	FP-LDA	6.111[2]	-	56 [2]	4.52 [2]
	FP-GGA	6.230 [2]	-	49 [2]	4.28 [2]
	PP-LDA	6.09 [30]	-	56 [30]	4.36 [30]
	PP-LDA	6.08 [3]	-	-	–
	HF	6.22 [31]	-	61 [31]	-
	HF	6.261 [32]	-	65 [32]	-
GaSb					
Present work	FPLAPW-GGA	6.214	405.318	44.498	4.549
	FPLAPW-LDA	6.050	374.003	55.039	4.877
Experiment	–	6.118 [29]	-	56 [29]	-
Other calculations	FP-LDA	6.053 [2]	-	54 [2]	4.26 [2]
	FP-GGA	6.219 [2]	-	45[2]	4.02 [2]
	LMTO-LDA	5.939 [33]	-	80 [33]	–
	PP-LDA	5.981 [30]	-	57 [30]	4.66 [30]
	PP-LDA	5.95 [3]	-	-	–
	HF	6.212 [32]	-	63 [32]	–
InSb					
Present work	FPLAPW-GGA	6.634	493.166	37.800	4.380
	FPLAPW-LDA	6.453	453.882	46.459	4.730
Experiment	-	6.478 [29]	-	46 [29]	-
Other calculations	FP-LDA	6.456 [2]	-	46 [2]	4.51 [2]
	FP-GGA	6.640 [2]	-	37 [2]	4.43 [2]
	PP-LDA	6.346 [30]	-	48 [30]	4.69 [30]
	HF	6.560 [31]	-	50 [31]	-
	HF	6.593 [32]	-	58 [32]	-

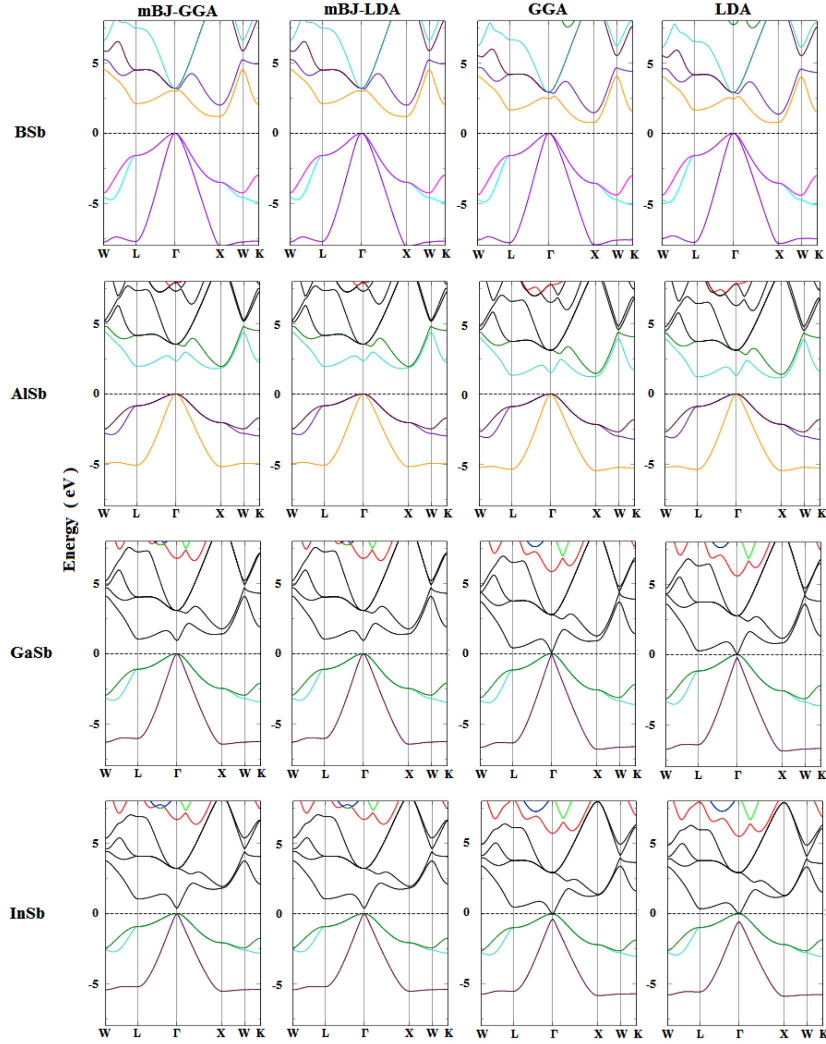

Fig. 1.Band structures Of BSb, AlSb, GaSb and InSb calculated within mBJ-GGA (a), mBJ-LDA (b), GGA (c) and LDA (d).

Table 2.The energy band gap (E_g) values of BSb, AlSb, GaSb, and InSb within LDA, GGA, mBJ-LDA and mBJ-GGA.

Compounds	Methods	XC	Eg (eV)	Type of band-gap
AlSb				
Present work	FP-LAPW	mBJ-GGA	1.804	Indirect(Γ-Δ_{min})
	FP-LAPW	mBJ-LDA	1.801	Indirect(Γ-Δ_{min})
	FP-LAPW	GGA	1.226	Indirect(Γ-Δ_{min})
	FP-LAPW	LDA	1.154	Indirect(Γ-Δ_{min})
Experiment			1.686 [29]	Indirect(Γ-Δ_{min})
Other calculations	FP-LAPW	GGA	1.214 [2]	Indirect(Γ-Δ_{min})
	FP-LAPW	LDA	1.141 [2]	Indirect(Γ-Δ_{min})
	FP-LAPW	GGA-EV	1.835 [2]	Indirect(Γ-Δ_{min})
	PP-PW	LDA	1.67 [30]	Indirect(Γ-Δ_{min})
BSb				
Present work	FP-LAPW	mBJ-GGA	1.136	Indirect(Γ-Δ_{min})
	FP-LAPW	mBJ-LDA	1.130	Indirect(Γ-Δ_{min})
	FP-LAPW	GGA	0.766	Indirect(Γ-Δ_{min})
	FP-LAPW	LDA	0.768	Indirect(Γ-Δ_{min})
Experiment			0.51 [35]	Indirect(Γ-Δ_{min})

Compounds	Methods	XC	Eg (eV)	Type of band-gap
Other calculations	FP-LAPW	GGA	0.763 [2]	Indirect(Γ-Δ_{min})
	FP-LAPW	LDA	0.751 [2]	Indirect(Γ-Δ_{min})
	FP-LAPW	GGA-EV	1.334 [2]	Indirect(Γ-Δ_{min})
	FP-LAPW	GGA	0.75 [28]	indirect (Γ-Δmin)
	LMTO	LDA	0.470 [33]	Direct (Γ- Γ)
	PP-PW	LDA	0.547 [30]	Direct (Γ- Γ)
GaSb				
Present work	FP-LAPW	mBJ-GGA	1.331	Direct (Γ- Γ)
	FP-LAPW	mBJ-LDA	1.320	Direct (Γ- Γ)
	FP-LAPW	GGA	0.025	Direct (Γ- Γ)
	FP-LAPW	LDA	0.000	Direct (Γ- Γ)
Experiment			0.670 [36]	Direct (Γ- Γ)
Other calculations	FP-LAPW	GGA	0.028 [2]	Direct (Γ- Γ)
	FP-LAPW	LDA	0.000 [2]	Direct (Γ- Γ)
	FP-LAPW	EVA	0.361 [2]	Direct (Γ- Γ)
	LMTO	LDA	0.470 [33]	Direct (Γ- Γ)
	PP-PW	LDA	0.547 [30]	Direct (Γ- Γ)
InSb				
Present work	FP-LAPW	mBJ-GGA	0.503	Direct (Γ- Γ)
	FP-LAPW	mBJ-LDA	0.501	Direct (Γ- Γ)
	FP-LAPW	GGA	0.000	Direct (Γ- Γ)
	FP-LAPW	LDA	0.000	Direct (Γ- Γ)
Experiment			0.2 [37]	Direct (Γ- Γ)
			0.25 [38]	Direct (Γ- Γ)
Other calculations	FP-LAPW	GGA	0.000 [2]	Direct (Γ- Γ)
	FP-LAPW	LDA	0.000 [2]	Direct (Γ- Γ)
	FP-LAPW	GGA-EV	0.200 [2]	Direct (Γ- Γ)
	FP-LAPW	LDA	−0.72 [39]	Direct (Γ- Γ)
	PP-PW	LDA	0.213 [30]	Direct (Γ- Γ)

Fig. 2 further explains the band gap, in which total density of states (TDOS) and atomic site projected densities of states (PDOS) of BSb, AlSb, GaSb and InSb with mBJ-GGA are plotted. We can specify the angular momentum character of different structures from PDOS. The Fermi level is set to be 0 eV. In case of mBJ-GGA, three different regions in DOS of these compounds appear separated from each other by gaps. Involvement of core state constitutes lower valence band while upper valence band starts from -14eV, -10.5eV, -11eV and 10.1 eV in case of BSb, AlSb, GaSb and InSb respectively. B-2p, Al-3p, Ga-4p, In-5p and Sb-5p states are main contributors in upper valence as well as in lower conduction band in their respective compounds. The second highest contribution is from B-2s, Al-3s, Ga-4s, In-5s and Sb-5s states. In case of AlSb localization of Al/Sb-s states is visible in between -5.2 eV and -4.9 eV. Another prominent localized region is also present in InSb (for Sb-s state) between -10.1eV to -9.8eV. Covalent interactions are present between the bonding elements due to degeneracy of states with regard to both lattice site and angular momentum.

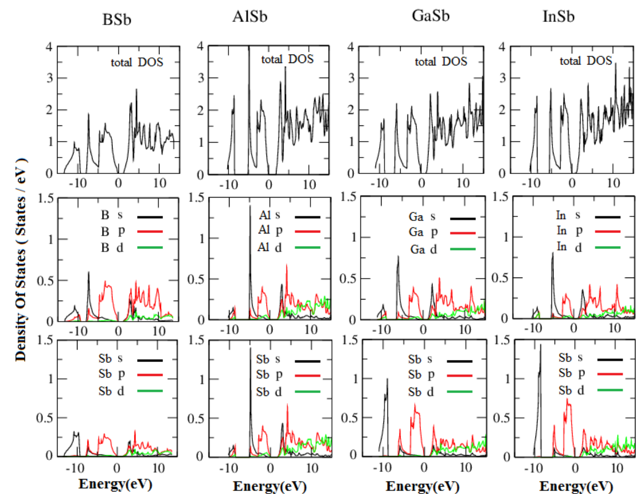

Fig. 2. Total and partial densities of states for BSb, AlSb, GaSb and InSb calculated within mBJ-GGA.

The contour and 3-D plot for electron density in the (110) plane are shown in Fig. 3. The plots are helpful to probing the bonding nature of constituent atoms. Plots show little ionic behaviour as there is diminutive difference of electronegativity between the comprising elements. Therefore, the bonding may be expressed as a

strong covalent behavior and BSb shows strongest covalent character in all of them. Ions in the lattice could diffuse in the vacant space (as shown in contour plot) having little localization of charge [40].

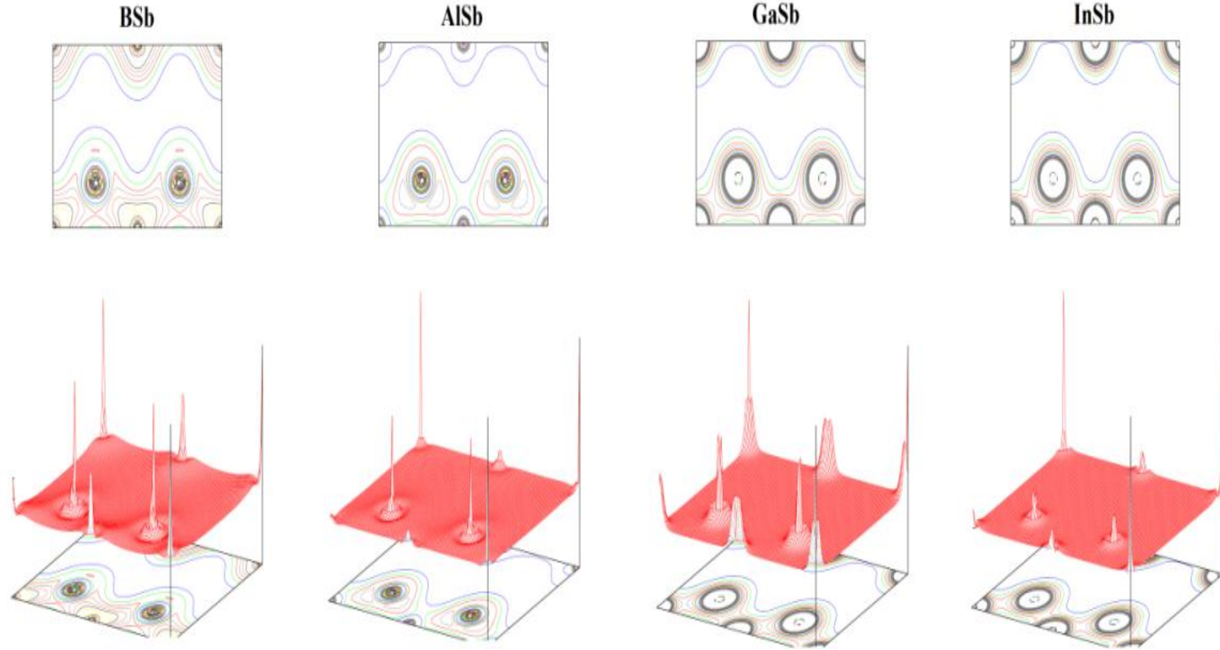

Fig. 3. The contour and 3D plots of BSb, AlSb, GaSb and InSb for electron density in the (110) plane.

For cubic symmetry compounds $\varepsilon_2(\omega)$ (imaginary part of the complex dielectric function) can be calculated by the following relation: [41]

$$\varepsilon_2(\omega)=\frac{8}{2\pi\omega^2}\sum_{nn'}\int_{BZ}\left|P_{nn'}(k)\right|^2\frac{dS_k}{\nabla\omega_{nn'}(k)} \quad (1)$$

Here $\omega_{nn'}$ is joint density of states and $P_{nn'}$ is momentum matrix element which affect $\varepsilon_2(\omega)$ strongly. Kramers-Kronig relation gives the real part of the complex dielectric function $\varepsilon_1(\omega)$ from the imaginary part $\varepsilon_2(\omega)$: [42]

$$\varepsilon_1(\omega)=1+\frac{2}{\pi}P\int_0^\infty\frac{\omega'\varepsilon_2(\omega')}{\omega'^2-\omega^2}d\omega' \quad (2)$$

The dielectric function's imaginary part is calculated in the energy range 0-30 eV for different exchange correlation functionals as shown in Fig.4. Transitions from top of the valence bands to conduction bands at the lower states, contribute to the major part of the optical spectra [43]. The first critical point (optical absorption's edge) in BSb, AlSb, GaSb and InSb occurs at about 1.136 eV, 1.804 eV, 1.331 eV, and 0.503 eV for mBJ-GGA. This point splits the valence band and conduction band at Γ point (Γ_V-Γ_C) which gives the threshold for direct optical transition between the highest valence band and the lowest conduction band. This is known as the fundamental absorption edge [44]. BSb, AlSb, GaSb and InSb have strong absorption in between energy range 3-8 eV, 2-7 eV, 1-7 eV, 1-7 eV respectively. This region is represented by different peaks due to electronic transitions between valence and conduction band. The absorption region has variation of the peak in the range of energy (as mentioned previously) that depicts the appropriateness for device applications as these compounds can be operated within diverse segments of the spectrum.

Computed real portion of dielectric function $\varepsilon_1(\omega)$ is shown in Fig. 5. Static dielectric constant $\varepsilon_1(0)$ and $\varepsilon_1(\omega)$ in low energy limit strongly rely on the band gap of the compound. Penn Model can be used to explain the inverse relation of $\varepsilon_1(0)$ with the band gap [45].

$$\varepsilon(0)\approx 1+(\hbar\omega_p/\mathrm{E}_g)^2 \quad (3)$$

Using the value of $\varepsilon_1(0)$ and plasma energy $\hbar\omega_p$ in above relation, the band gap value E_g can be calculated. The static dielectric constant values of BSb, AlSb, GaSb and InSb, measured with mBJ-GGA exchange correlations are listed in Table.3. With mBJ-GGA, it is clear from Fig. 6 that $\varepsilon_1(\omega)$ increases initially with energy reaching at maximum value at 3.2 eV, 2.7 eV, 1.9 eV and 1.8 eV for BSb, AlSb, GaSb and InSb respectively and afterward lowers to a smallest (negative) value at 6.4 eV, 4.2 eV, 4.1 eV and 5.2 eV for BSb, AlSb, GaSb and InSb respectively. The values lower than one for $\varepsilon_1(\omega)$ exhibit the reflectiveness of material for the incident waves

(electromagnetic) inside this energy range displaying a metallic character. So protection from radiations is possible in specific energy limits. The local maxima of reflectivity as shown in Fig. 7 correspond to the negative values of $\varepsilon_1(\omega)$. Additional increase in energy to high value brings stability to $\varepsilon_1(\omega)$. Materials show steady character after 10 eV which suggests that the considered compounds behave as transparent and are suitable for making lenses. Photons with energy greater than 10 eV do not interact with materials.

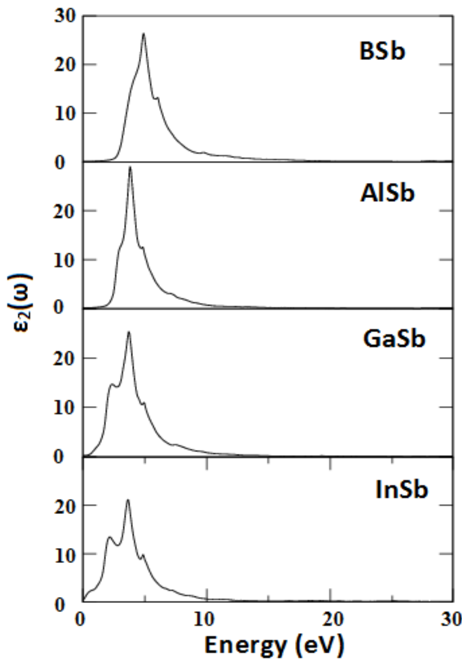

Fig. 4. Frequency dependent imaginary part of dielectric function of BSb, AlSb, GaSb and InSb within mBJ-GGA.

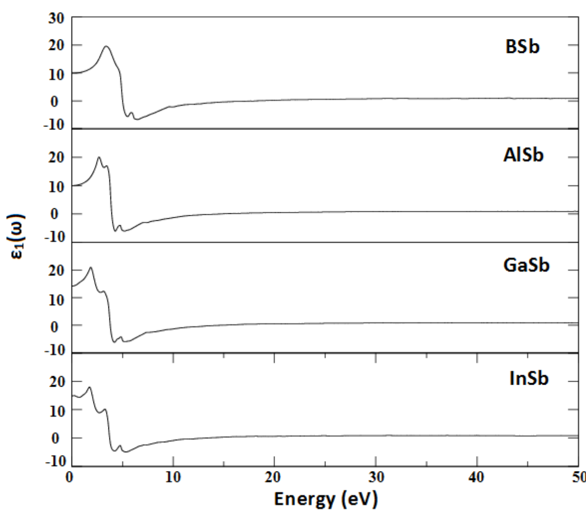

Fig. 5. Frequency dependent real part of dielectric functions of BSb, AlSb, GaSb and InSb within mBJ-GGA.

Table 3. Calculated static dielectric constant $\varepsilon_1(0)$, static refractive index n(0) for BSb, AlSb, GaS band InSb within mBJ-GGA.

Compound	Method	XC	$\varepsilon_1(0)$	n(0)
BSb	FP-LAPW	mBJ-GGA	9.897	3.146
AlSb	FP-LAPW	mBJ-GGA	9.986	3.160
GaSb	FP-LAPW	mBJ-GGA	14.1798	3.76573
InSb	FP-LAPW	mBJ-GGA	14.8552	3.84817

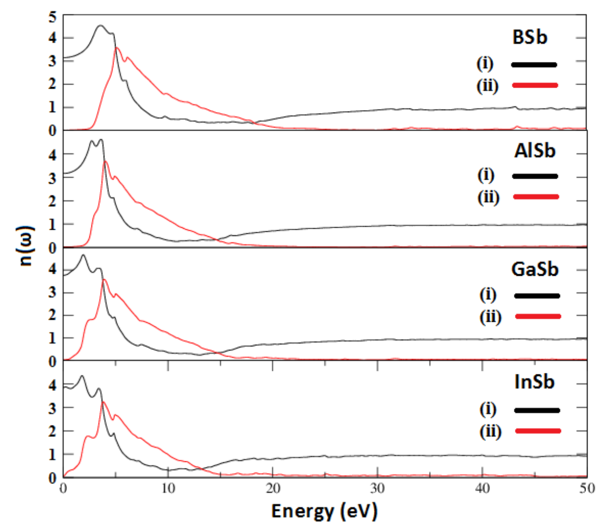

Fig. 6. Frequency dependent (i) refractive index (ii) extinction coefficient of BSb, AlSb, GaSb and InSb within mBJ-GGA.

Fig. 6(i) shows the refractive index $n(\omega)$over a broad spectrum for longer range of energy (0-50eV). The spectrum of refractive index $n(\omega)$ closely follows to real part of the complex dielectric function $\varepsilon_1(\omega)$ [46]. Refractive index spectra of III-Antimonides show two significant features. The figure shows that $n(\omega)$ reaches the highest value at around 4.5 at 3.5 eV , 4.6 at 3.6 eV, 4.65 at 2 eV and 4.35 at1.7 eV for BSb, AlSb, GaSb and InSb respectively with mBJ-GGA. Afterwards spectrum of $n(\omega)$ decrease at intermediate energies and then vanishes at higher energies. This is due to the absorbance of high energy photons by materials and no more act as transparent. In Figure 6(i) refractive index drops down to less than one for small range of energy. This depicts the lower value of *c* (celerity of light) than the *v* (phase velocity of light) that seems contradiction to the relativity. The signal is considered to transmit with group velocity v_g

($v_g = \frac{d\omega}{dk}$) through medium of dispersive nature instead with phase velocity ($v = \frac{\omega}{k} = \frac{c}{n}$). The relation between v_g and v is given by:

$$v_g = v(1 - \frac{k}{n}\frac{dn}{dk}) \qquad (4)$$

Eq.4 suggests that v is always greater than v_g. When a signal having v greater than c, propagates through spectral region then c is always greater than v_g [46]. The static refractive index $n(0)$ values with mBJ-GGA are listed in Table 3.

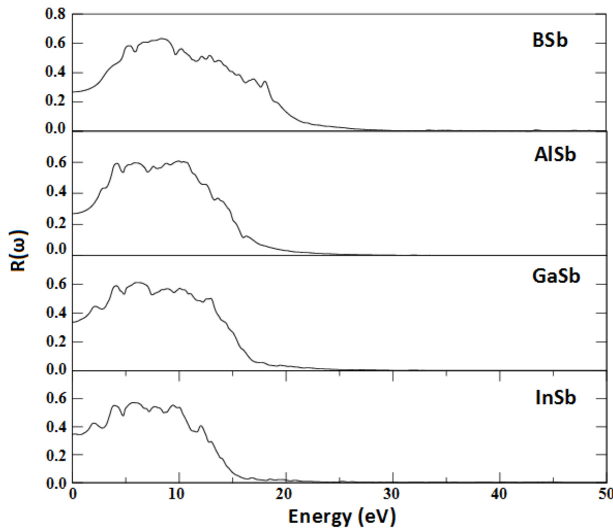

Fig. 7. Reflectivity (frequency dependent) of BSb, AlSb, GaSb and InSb within mBJ-GGA.

Extinction coefficient $k(\omega)$ along with energy is shown in Fig.6 (ii). The response of both $k(\omega)$ and $\varepsilon_2(\omega)$ with energy is similar which is also indicated by existing theory [46]. But a material with some coefficient of absorption does not fallow this trend and $k(\omega)$ shows some deviation from $\varepsilon_2(\omega)$[46].

Fig. 7 shows frequency dependent $R(\omega)$ against energy with mBJ-GGA. At zero frequency the magnitude of coefficient of reflectivity for BSb, AlSb, GaSb and InSb are 0.268, 0.270, 0.337 and 0.345 respectively. Peaks pointing (arises from the inter band transition) maximum value of reflectivity lies in the energy range of 6-9 eV (BSb), 4-11eV (AlSb), 4-10.2 eV (GaSb) and 3.6-10eV (InSb). Protection from rays is possible in this energy range. The maximum value of reflectivity appears at about 8.3 eV (BSb), 10 eV (AlSb), 5.9 eV (GaSb) and 5.8 eV (InSb). Considered III-Antimonides have reflectivity over broader range of energy which is desirable for reflectors.

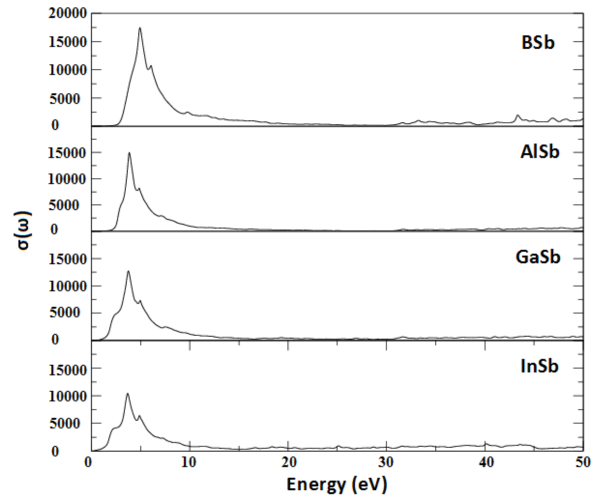

Fig. 8. Optical conductivity (frequency dependent) of BSb, AlSb, GaSb and InSb within mBJ-GGA.

Fig. 8 shows the frequency dependent optical conductivity σ(ω) for III-Antimonides. The variation of frequency is described by energy (0 to 50 eV) and the σ(ω) is given in the units of $\Omega^{-1}cm^{-1}$. With small energy range, under studied compounds depict sharp rise in conductivity attaining maximum value at around 4.9 eV, 3.8 eV, 3.7 eV, 3.7 eV for BSb, AlSb, GaSb and InSb respectively. After reaching the highest value, conductivity drops down quickly within small energy range in all of the considered cases. For the high energy range, negligible amount of conductivity is noticeable which shows that materials do not correspond to interactive photons.

4. Conclusions

Optoelectronic properties of X-Sb (B, Al, Ga, In) have been studied with modified Becke Johnson potential. With mBJ-GGA our predicted band gap values for BSb (1.136 eV) & AlSb (1.804 eV) show very close agreement with values calculated with EV-GGA, whereas the band gap values for GaSb (1.331 eV) & InSb (0.503 eV) are enhanced as compare to the previous calculated results including LDA/GGA/EV-GGA depicting the true nature of these compounds. Optical parametric quantities (refractive index, dielectric constant, reflectivity and optical conductivity) which depend on band gap are presented and discussed. Strong absorption is noted between energy range 3-8 eV, 2-7 eV, 1-7 eV and 1-7 eV for BSb, AlSb, GaSb and InSb respectively. The values for static dielectric constant for BSb, AlSb, GaSb and InSb are 9.897, 9.986, 14.1798 and 14.8552 respectively. The values of calculated static refractive index are 3.146, 3.160, 3.76573 and 3.84817 for BSb, AlSb, GaSb and InSb respectively. Conductivity of the entire considered material rises sharply with small energy change. Considered materials show reflective character for electromagnetic incident waves when value for $\varepsilon_1(\omega)$ drops lower than one and thus protection from radiations is

possible in specific energy limits. Our results for band gap and optical parameters can be used productively in optoelectronic applications.

Acknowledgments

The authors would like to thank for the financial support (Foreign Academic Visitor Grant) of Universiti Teknologi Malaysia (UTM) Skudai, Johor, Malaysia for the grant No. JI3000077264D035 for this research work.

References

[1] I. Vurgaftman, J. R. Meyer, L. R. Ram-Mohan, J. Appl. Phys. 5815 (2001).
[2] R. Ahmed, Fazal-e-Aleem, S. J. Hashemifar, H. Rashid, H. Akbarzadeh, Commun. Theor. Phys. **52**, 527 (2009).
[3] H. Zhu-Feng, Z. Zi-Zhong, H. Mei-Chum, Y. Yong, Phys. Chem. Commun. **6**, 47 (2003).
[4] J. T. Vaughey, J. O. Hara, M. M. Thackeray, Electrochem.Solid State Lett.**3**, 13(2000).
[5] J. T. Vaughey, C. S. Johnson, A. J. Kropf, R. Benedek, M. M. Thackeray, H. Tostmann, T. Sarakonsri, S. Hackney, L. Fransson, K. Edstr¨om, J. O. Thomas, J. Power Sources **97-98**, 194 (2001).
[6] A. J. Kropf, H. Tostmann, C. S. Johnson, J. T. Vaughey, M. M. Thackeray, Electrochem. Commun. **3**, 244 (2001).
[7] K. C. Hewitt, L. Y. Beaulieu, J. R. Dahn, J. Electrochem. Soc. **148**(5), A402 (2001).
[8] R. Benedek, J. T. Vaughey, M. M. Thackeray, L. H. Yang, R. Prasad, J. Power Sources **97-98**, 201 (2001).
[9] M. Wachtler, M. Winter, J. O. Besenhard, J. Power Sources **105**, 151 (2002).
[10] GokhanGoko˘glu, Journal of Alloys and Compounds **478**, 653 (2009).
[11] U. Ro¨ssler, Solid State Commun. **49**, 943 (1984).
[12] K. M. Yu, A. J. Moll, N. Chan, W. Walukiewiez, P. Bala, App. Phys. Lett. **66**, 2406 (1995).
[13] T. Singh, R. K. Bedi, Thin Solid Films **312**,111 (1998).
[14] J. P. Perdew, Y. Wang, Phys. Rev. B **45**, 13244 (1992).
[15] Perdew, K. Burke, M. Emzerhof, Phys. Rev. Lett. **77**, 3865 (1996).
[16] D. Koller, F. Tran, P. Blaha, Phys. Rev. B **83**, 195134 (2011).
[17] E. Engel, Phys. Rev. B **80**, 161205 (2009).
[18] V. I. Anisimov, J. Zaanen, O. K. Andersen, Phys. Rev. B **44**, 943 (1991).
[19] F. Tran, P. Blaha, Phys. Rev. Lett. **102**, 226401 (2009).
[20] M. Yousaf, M. A. Saeed, A. R. M. Isa, A. Shaari, H. A. R. Aliabad, Chin. Phys. Lett. **29**, 107401 (2012).
[21] M. Yousaf, M.A. Saeed, R. Ahmed, M.M. Alsardia, A. R. M. Isa, A. Shaari, Commun. Theor. Phys. (In Press).
[22] W. Kohn, L. S. Sham, Phys. Rev. **140**, A1133 (1965).
[23] P. Blaha, K. Schwarz, G. Madsen, D. Kvasnicka, J. Luitz, Institute of Material Chemistry, TU Vienna. http://www.wien2k.at/.
[24] F. Zerarga, A. Bouhemadou, R. Khenata, S. Bin-Omran, Solid State Sci. **13**, 1638(2011) and references therein.
[25] F. D. Murnaghan, Proc. Nat. Acad. Sci. USA **30**, 244 (1944).
[26] M. Ferhat, B. Bouhafs, A. Zaoui, H. Aourag, J. Phys.: Condens. Matter **10**, 7995 (1998).
[27] B. Bouhafs, H. Aourag, M. Cartier, J. Phys. Matter **12**, 5655 (2000).
[28] A. Zaoui, F. El. Haj Hassan, J. Phys.: Condens. Matter **13**, 253 (2001).
[29] R. W. G. Wyckoff, Crystal Structures, 2nd Edition, Krieger, Malabar (1986); O. Madelung, Semiconductors: Data Handbook, Springer, Berlin (2004); O. Madelung, Numerical data and Functional Relationships in Science and Technology, Springer, Berlin (1982); http://cstwww.nrl.navy.mil/lattice/.
[30] S. Q. Wang, H. Q. Ye, J. Phys.: Condens. Matter **14**, 9579 (2002).
[31] M. Causa, R. Dovesi, C. Roetti, Phys. Rev. B **43**, 11937 (1991).
[32] S. Kalvoda, B. Paulus, P. Fulde, H. Stoll, Phys. Rev. B **55**, 4027 (1997).
[33] B. K. Agrawal, P. S. Yadav, S. Kumar, S. Agrawal, Phys. Rev. B **52**, 4896 (1995).
[34] B. Amin, I. Ahmad, M. Maqbool, S. Goumri-Said, R. Ahmad, J. Appl. Phys. **109**, 023109 (2011).
[35] S. Hussain, S. Dalui, R. K. Roy, A.K. Pal, J. Phys. D: Appl. Phys. **39**, 2053 (2006).
[36] R. C.Weast, D. R. Lide, M. J. Astle, W. H. Beyer, CRC Handbook of Chemistry and Physics, 70th Edition edited by CRC, Boca Ratom, Florida 1990.
[37] I. Vurgaftman, J. R. Meyer, L. R. Ram-Mohan, J. Appl. Phys. **89**, 5815 (2001); references therein; A. Mujica, Angel Rubio, A. Munoz, R.J. Needs, Rev. Mod.Phys. **75**, 863 (2003); references therein; G.J. Ackland, Rep. Prog. Phys. **64**,483(2001); references therein.
[38] Alan Owens, A. Peacock, Nuclear Instruments and Methods in Physics Research A **531**, 18(2004).
[39] R. Ashi, W. Mannstadt, A. J. Freeman, Phys. Rev. **59**, 7486 (1999).
[40] Y. -N. Xu, W. Y. Ching, Phys. Rev. B **43**, 4461 (1991).
[41] B. Amin, I. Ahmad, M. Maqbool, S. Goumri-Said, R. Ahmad, J. Appl. Phys. **109**, 023109 (2011).
[42] F. Wooten, Optical Properties of Solids, Academic Press, New York 1972.
[43] N. J. Van der Laag, M. D. Snel, P. C. M. Magusin, G. de With, J. Eur. Ceram. Soc. **24**, 2417 (2004).
[44] D. Allali, A. Bouhemadou, S. Bin-Omran, Comp. Mater. Sci. **51**, 194 (2011).
[45] D. Penn, Phys. Rev. **128**, 209 3(1962).
[46] M. Fox, Optical Properties of Solids; Oxford University Press: Oxford, U.K., 2001.

* Correspondence author: saeed@utm.my